Measurement of Absolute Cross Sections for Excitation of the $3s^2 3p^5\ ^2P^o_{3/2}$-$3s^2 3p^5\ ^2P^o_{1/2}$ Fine-Structure Transition in Fe^{9+}

M. Niimura, I. Čadež,* S. J. Smith, and A. Chutjian

Jet Propulsion Laboratory, California Institute of Technology, Pasadena, California 91109

(Received 6 November 2001; published 20 February 2002)

Experimental cross sections are reported for the $3s^2 3p^5\ ^2P^o_{3/2}$-$3s^2 3p^5\ ^2P^o_{1/2}$ transition in Fe^{9+} located at 1.945 eV. The center-of-mass interaction energies are in the range of 1.72 eV (below threshold) through threshold, to 5.6 eV (2.9×threshold). Data are compared with results of a 49-state Breit-Pauli R-matrix theory. The experiment detects structures at 3.5 and 4.6 eV corresponding to enhancement of the direct excitation via many narrow, closely spaced resonances about these energies calculated by the theory. Iron is present in practically every astrophysical object, as well as being an impurity in fusion plasmas. Present data are the first electron-energy-loss measurements on a highly charged iron ion.

DOI: 10.1103/PhysRevLett.88.103201 PACS numbers: 34.80.Kw

The ground-state fine-structure transition $3p^5\ ^2P^o_{3/2} \rightarrow 3p^5\ ^2P^o_{1/2}$ in Fe^{9+} can be observed over the cool solar corona ($T \approx 2 \times 10^6$ K) and in sunspot regions ($T \approx 4 \times 10^6$ K). In general, the lines in Fe IX–Fe XIV are important diagnostics of the electron temperature (T_e) and density (N_e) in different solar regions and features. A summary of the use and theory of this so-called coronal red line can be found in Mason [1].

In order to convert line intensities to actual T_e and N_e, one needs reliable theoretical or experimental data. For almost all ion species, and for practically all charge states and transitions, only theoretical data are available, with no comparison to absolute, or even normalized, experimental cross sections. Presented herein are first experimental measurements of absolute collisional excitation cross sections in a highly charged iron ion, for the $^2P^o_{3/2} \rightarrow {}^2P^o_{1/2}$ transition in Fe^{9+}. Comparison is given with the recent results of Tayal [2,3] in a 49-state Breit-Pauli R-matrix calculation for this transition.

The experimental measurements were carried out using the 14.0 GHz electron cyclotron resonance (ECR) ion source at the JPL Highly Charged Ion (HCI) Facility [4–6]. The $^{56}Fe^{9+}$ ions were generated from ferrocene vapor, and extracted at 9×6.4 keV from the ECR source. The metastable fraction was determined using the gas-attenuation technique [7]. The fraction was determined for the different daily ECR running conditions, and applied to the measured cross sections. Ferrocene is an iron biphenyl compound [dicyclopentadienyl iron, $Fe(C_5H_5)_2$], and is a convenient method for generating Fe in the vapor state without use of a high-temperature oven to evaporate Fe directly [8]. Using ferrocene vapor directly introduced into the ECR plasma chamber, we were able to generate charge states of up to Fe^{15+} with 100 W microwave power. Higher charge states can almost certainly be generated at higher powers.

Experimental methods, and data acquisition and analysis methods, may be found in Refs. [6,9]. Briefly, use is made of the electron-energy-loss method, and merged beams of low-energy electrons and Fe^{9+} ions. The various Fe^{q+} charge states from ECR plasma ions are mass/charge analyzed in a double-focusing 90° bending magnet. The Fe^{9+} beam is focused into the center of the interaction region, where it interacts with a magnetically confined electron beam which is merged with the ions through a trochoidal analyzer. The electrons and ions interact along a 20.0 ± 0.3 cm path length. After the interaction, the electrons are demerged from the ions using a second trochoidal analyzer. Detection is by means of a position-sensitive detector at the exit of the second trochoidal system. Beam profiles are measured at four locations along the merged path using vanes with circular holes that intersect the merged beams at different radial distances. An electronic aperture [5] is used to discriminate against elastically scattered electrons prior to the trochoidal electron-energy-loss analyzer; and retarding grids are used after the analyzer. Small, remnant background signals from elastically scattered electrons which may overlap the inelastic spectrum are accounted for through the use of trajectory modeling and calculated elastic differential cross sections. These three features, combined with the velocity dispersion of the trochoidal monochromator, allow one to carry out measurements at energies from threshold to approximately 3 times threshold.

The relation between experimentally measured quantities and the cross section $\sigma(E)$ (cm^2) for excitation at center-of-mass (CM) energy E is given by

$$\sigma(E) = \frac{\mathbb{R} q e^2 \mathcal{F}}{\varepsilon I_e I_i L} \left| \frac{v_e v_i}{v_e - v_i} \right|, \qquad (1)$$

where $\mathbb{R}$ is the total signal rate (s^{-1}), q is the ionic charge state, e is the electron charge (C), I_e and I_i are the electron and ion currents (A), respectively, v_e and v_i are the electron and ion velocities ($cm\,s^{-1}$), respectively, L is the merged path length (cm), ε is the efficiency of the combined rejection grids/microchannel-plate detection system (dimensionless), and $\mathcal{F}$ is the overlap factor between the electron and ion beams (cm^2).

All quantities in Eq. (1) are measured, or in the case of the particle velocities are known nominally through their acceleration potentials. There are errors associated with their measurements. The sources of these errors have been discussed in Ref. [10]. A listing of the experimental parameters, and their errors, is given here in Table I. The entries "metastable fraction" and "overlapping elastic contribution" perhaps require more explanation. Knowledge of the fraction of Fe^{9+} ions in metastable states is important in that excitation events out of metastable levels are *not* counted in the rate $\mathbb{R}$, but the metastable current *is* counted in I_i. Using the beam-attenuation method [7,11], the Fe^{9+} metastable fraction was measured daily prior to the start of measurements, after the ion source was tuned and stabilized. The error estimate (3.0%) is based on the average of these repeated measurements, and the scatter in the slopes of the beam-attenuation plots. Elastic electron scattering from HCIs scales as the square of the ion charge, and hence is 81 times more intense for Fe^{9+} than for O^+, for example. The error estimate of the overlapping elastic contribution (7.0%) is determined by the ability of the electronic aperture to reject the larger Larmor-radius electrons, the ability of the retarding grids to reject forward-scattered electrons, and the estimated error incurred in modeling the remaining high-angle, elastically scattered electrons using angular distributions from phase-shift calculations [10]. The error in the measurements *below* threshold is a conservative estimate of the error encountered in subtracting a small, residual elastic contribution to the total inelastic scattering. The error bars on the final data represent 1–5 independent measurements at each CM energy.

The electron-energy scale was calibrated at several times: one month prior to all measurements, and two weeks after. Use was made of the retarding potential difference method with the grids in front of the position-sensitive detector (PSD). In both cases, there was the same 1.0 ± 0.1 V offset between the nominal cathode bias voltage and the grid cutoff voltage. This offset and the spectroscopic energy onset of the signal were used to fix the energy scale with a 0.1 eV error. The resolution of the electron beam (100 meV, FWHM) was unchanged from previous measurements.

TABLE I. Individual and total-quadrature experimental uncertainties in the e-Fe^{9+} cross sections, for a single measurement at a given energy.

Source of uncertainty	Uncertainty (1σ confidence level) (%)
Counting statistics	1.0
Form factor	6.0
Path length	1.0
Electron-current measurement	0.5
Ion-current measurement	0.5
PSD efficiency calibration	1.5
Overlapping elastic contribution	7.0
Overlapping inelastic contribution	3.0
Metastable fraction	3.0
Total quadrature uncertainty (1.7σ or 90% C.L.)	18%

The excitation of positive ions is often dominated at threshold by resonances, most of which are too narrow to be resolved with the present experimental resolution. Hence, one must often measure a cross section averaged over these sharp structures. Even so, enhancements are clearly detected in the measured cross sections. If we denote the laboratory energies of the electrons and the Fe^{9+} ions as E_e and E_i, their masses as m_e and m_i, respectively, and the reduced mass as μ, the expression for the CM energy E in Eq. (1) in terms of the laboratory (LAB) energies is just

$$E = \mu\left[\frac{E_e}{m_e} + \frac{E_i}{m_i} - 2\left(\frac{E_e E_i}{m_e m_i}\right)^{1/2}\cos\vartheta\right], \qquad (2)$$

where ϑ is the LAB angle between the electron and the ion beams, and is taken as 0° here. In addition to displaying the energetics of the scattering, Eq. (2) is useful for calculating the expected behavior of the CM *resolution*, especially as a function of the LAB electron energy E_e. To show this, one takes the partial derivative of Eq. (2) with respect to E_e, uses finite differentials, and sets $\mu = m_e$ to obtain

$$\Delta E = \Delta E_e\left[1 - 3.1203 \times 10^{-3}\left(\frac{E_i}{E_e}\right)^{1/2}\right]. \qquad (3)$$

Here, ΔE is the energy width in the CM frame, and ΔE_e is the electron energy width in the LAB frame.

Results of the 49-state Breit-Pauli R-matrix calculations [3] are shown in Fig. 1. These theoretical results were convoluted with the energy-dependent width of Eq. (3) using a measured laboratory electron-energy resolution of

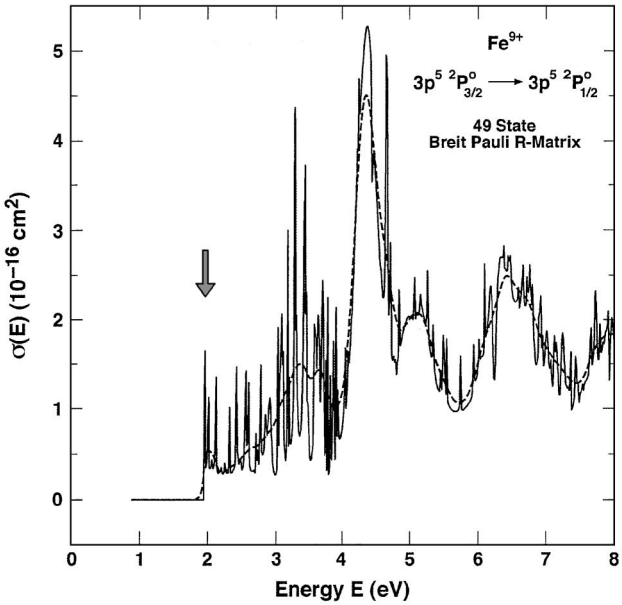

FIG. 1. Overlay of the results of the 49-state Breit-Pauli calculations of Ref. [3] (solid line) with their values as convoluted with an electron-energy width $\Delta E_e = 100$ meV using Eq. (3) (dashed line). The arrow denotes the threshold for the transition at 1.945 eV.

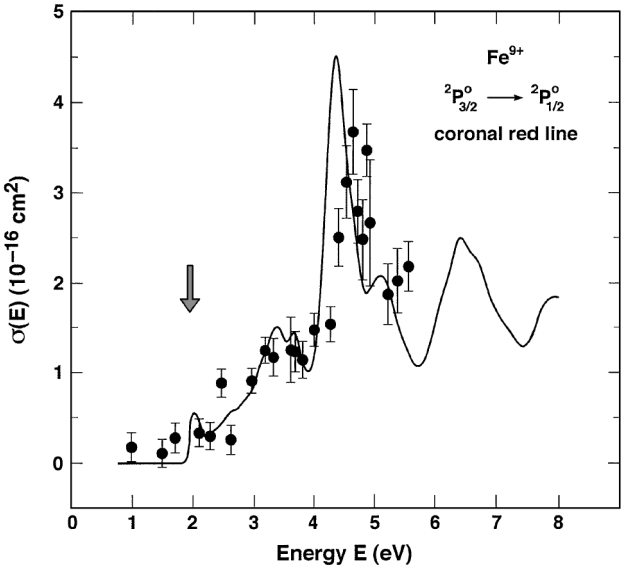

FIG. 2. Comparison of the convoluted 49-state Breit-Pauli R-matrix results (solid line) and measured absolute experimental cross sections (solid circles) for the Fe^{9+} coronal red-line transition (λ6376 Å). Experimental errors are shown at the 1.7σ (90%) confidence level. This is 18% or less, depending on the number of measurements (1–5) of each cross section. The energy scale is accurate to 0.1 eV, and the vertical arrow denotes the transition threshold at 1.945 eV.

$\Delta E_e = 100$ meV [10]. These results are also shown in Fig. 1. While the effect of the convolution is certainly to smooth over most of the relatively sharp, weak resonances, several notable features remain, especially peaks at 3.5 eV, 4.35 eV, and a shoulder at 5.2 eV. Shown in Fig. 2 is a comparison of the convoluted theoretical results with the present experimental cross sections (the latter listed in Table II). One sees that experiment and theory confirm the strong resonance. The calculated peak location is 4.35 eV, and the measured location is 4.6 ± 0.1 eV. This corresponds to a slight shift of the resonances to a higher energy in the experiment. However, agreement with theory is quite reasonable, considering the combined experimental error (0.1 eV), and the uncertainties in the results of theory arising from the number and the type of bound and continuum orbitals, choice of boundary radii, and the description of electron correlation and relativistic effects. Energy, differences of the order of 0.2 eV (0.015 Ry) do not significantly alter the effective collision strengths often used in astrophysics, as these quantities are averages over a much broader electron-energy width.

One also detects in the measurements evidence for the weaker resonances at 3.5 eV and the shoulder at 5.2 eV. However, these features are relatively broad and weak for an energy-scale comparison.

The present results on Fe^{9+} represent the first experimental data on excitation cross sections in a highly charged iron ion. Iron is present throughout the universe, in stars, our Sun, and in the interstellar medium. It is also a significant impurity in high-electron temperature plasmas such as the tokamak, the Joint European Torus, and the upcoming International Thermonuclear Experimental Reactor. As such, work is underway at JPL/Caltech to measure excitation cross sections in a series of Fe charge states, for the lower-lying energy levels, covering the energy range from threshold to approximately 3–5 times the threshold energy.

TABLE II. Experimental cross sections for the $3s^2 3p^5\ ^2P^o_{3/2}$-$3s^2 3p^5\ ^2P^o_{1/2}$ transition in Fe^{9+}. The experimental error is 18% (90% C.L.) or less, depending on the number of measurements at each energy. The excitation threshold is 1.945 eV.

Energy (eV)	Cross section (10^{-16} cm^2)
1.04	0.16
1.52	0.09
1.71	0.26
2.12	0.32
2.28	0.28
2.46	0.87
2.62	0.25
2.95	0.90
3.17	1.23
3.32	1.16
3.61	1.24
3.68	1.22
3.82	1.13
3.99	1.47
4.26	1.53
4.40	2.51
4.52	3.12
4.62	3.68
4.70	2.79
4.79	2.48
4.84	3.48
4.91	2.67
5.21	1.86
5.36	2.02
5.55	2.18

I. Čadež and M. Niimura thank the National Research Council. This work was carried out at the Jet Propulsion Laboratory, California Institute of Technology, and was supported under contract with the National Aeronautics and Space Administration.

*Permanent address: J. Stefan Institute, Ljubljana, Slovenia.

[1] H. E. Mason, At. Data Nucl. Data Tables **57**, 305 (1994).
[2] S. S. Tayal, Astrophys. J. Suppl. Ser. **132**, 117 (2001).
[3] S. S. Tayal, Astrophys. J. **544**, 575 (2000).
[4] A. Chutjian, J. B. Greenwood, and S. J. Smith, in *Applications of Accelerators in Research and Industry,* edited by J. L. Duggan and I. L. Morgan (American Institute of Physics, New York, 1999).
[5] J. B. Greenwood, S. J. Smith, A. Chutjian, and E. Pollack, Phys. Rev. A **59**, 1348 (1999).
[6] J. A. Lozano *et al.,* Phys. Rev. A **63**, 042713 (2001).
[7] C. Liao *et al.,* Astrophys. J. **484**, 979 (1997).
[8] H. Koivisto, J. Ärje, and M. Nurmia, Nucl. Instrum. Methods Phys. Res., Sect. B **94**, 291 (1994).
[9] J. B. Greenwood, S. J. Smith, and A. Chutjian, Phys. Rev. A **59**, 1348 (1999).
[10] S. J. Smith *et al.,* Astrophys. J. **541**, 501 (2000).
[11] S. J. Smith *et al.,* Astrophys. J. **463**, 808 (1996).